



Direct powder extrusion 3D printing: Fabrication of drug products using a novel single-step process



Alvaro Goyanes^{a,b,*}, Nour Allahham^{a,1}, Sarah J. Trenfield^{a,c}, Edmont Stoyanov^d,
Simon Gaisford^{a,c}, Abdul W. Basit^{a,c,*}

^a FabRx Ltd., 3 Romney Road, Ashford, Kent TN24 0RW, UK

^b Departamento de Farmacología, Farmacia y Tecnología Farmacéutica, R+D Pharma Group (GI-1645), Universidade de Santiago de Compostela, 15782, Spain

^c UCL School of Pharmacy, University College London, 29-39 Brunswick Square, London WC1N 1AX, UK

^d Nisso Chemical Europe GmbH, Berliner Allee 42, 40212 Dusseldorf, Germany

ARTICLE INFO

Keywords:

Three dimensional printing
Fused deposition modeling
Pellet extruder
Printing pharmaceuticals
Additive manufacturing
Oral medicinal dosage forms
Personalized medicines

ABSTRACT

Three-dimensional (3D) printing is revolutionising how we envision manufacturing in the pharmaceutical field. Here, we report for the first time the use of direct powder extrusion 3D printing: a novel single-step printing process for the production of printlets (3D printed tablets) directly from powdered materials. This new 3D printing technology was used to prepare amorphous solid dispersions of itraconazole using four different grades of hydroxypropylcellulose (HPC – UL, SSL, SL and L). All of the printlets showed good mechanical and physical characteristics and no drug degradation. The printlets showed sustained drug release characteristics, with drug concentrations higher than the solubility of the drug itself. The printlets prepared with the ultra-low molecular grade (HPC – UL) showed faster drug release compared with the other HPC grades, attributed to the fact that itraconazole was found in a higher percentage as an amorphous solid dispersion. This work demonstrates the potential of this innovative technology to overcome one of the major disadvantages of fused deposition modelling (FDM) 3D printing by avoiding the need for preparation of filaments by hot melt extrusion (HME). This novel single-step technology could revolutionise the preparation of amorphous solid dispersions as final formulations and it may be especially suited for preclinical studies, where the quantity of drugs is limited and without the need of using traditional HME.

1. Introduction

Three-dimensional printing (3DP) is an innovative technology that can convert 3D computer models into real objects by additive manufacturing (Basit and Gaisford, 2018). 3DP technologies have been available since the early 1990s, when they were developed for rapid and economic production of prototype models (Barnatt, 2016). The importance and relevance of 3DP for pharmaceutical applications have been extensively discussed elsewhere (Alhnan et al., 2016; Awad et al., 2018a; Goole and Amighi, 2016; Palo et al., 2017; Trenfield et al., 2018a,b, 2019; Zema et al., 2017) as an enabling technology to produce patient-tailored medicines (Pietrzak et al., 2015), to engineer drug release profiles from dosage forms (Fina et al., 2018a,b; Goyanes et al., 2015c; Martinez et al., 2018) and to deliver multiple drugs (Awad et al., 2019; Khaled et al., 2015a,b; Robles-Martinez et al., 2019).

There are a number of 3D printing technologies and variations,

which according to the 3D printing classification of the American Society for Testing and Materials (ASTM) can be classified into seven categories: Vat Photopolymerisation, Material Jetting, Binder Jetting, Material Extrusion, Powder Bed Fusion, Sheet Lamination and Directed Energy Deposition (ASTM, 2012; Madla et al., 2018). Among these 3DP technologies, material extrusion (in particular fused deposition modelling; FDM) is the most commonly used in pharmaceutical sciences due to the wide availability and low cost of the printers (Awad et al., 2018b; Goyanes et al., 2015b). In vivo studies on FDM 3D printed products have already been performed in animals (Arafat et al., 2018a; Genina et al., 2017; Goyanes et al., 2018) and in humans showing good acceptability (Goyanes et al., 2017b; Liang et al., 2018). FDM 3DP involves heating and extruding a drug-loaded polymer filament, normally prepared using hot melt extrusion (HME), through a nozzle tip followed by cooling-solidification onto a build plate into the selected shape (Vithani et al., 2019).

* Corresponding authors at: FabRx Ltd., 3 Romney Road, Ashford, Kent TN24 0RW, UK.

E-mail addresses: a.goyanes@fabrx.co.uk (A. Goyanes), a.basit@ucl.ac.uk (A.W. Basit).

¹ These authors contributed equally to this work.

FDM 3DP allows the preparation of solid dispersions and solutions (Alhijaj et al., 2016) via the dispersion or dissolution of drug in the polymer matrix, making it especially suitable for drugs with low water solubility and good thermal stability. Many polymers have been tested in HME + FDM 3DP (Melocchi et al., 2016), including hydroxypropyl cellulose (HPC) which is one of the most widely used polymers due to its suitable mechanical properties and ease of extrusion (Arafat et al., 2018b; Goyanes et al., 2017b; Pietrzak et al., 2015). Itraconazole is one example of a drug that could benefit from this technology to increase drug solubility and drug bioavailability via creation of a solid dispersion. Itraconazole is a BCS Class II wide spectrum antifungal agent, with a very low water solubility (1–4 µg/mL) and a melting point of 166–167 °C. It is commercially available in a fixed dosage strength of 100 mg or in a solution of 10 mg/mL which exhibit different oral bioavailabilities depending on the specific formulation (Barone et al., 1993). The evidence for the potential clinical benefits of drug monitoring and dose adjustment for patients receiving itraconazole is strong, and dose adjustment for renal impairment depending on creatinine clearance is often required (Ashbee et al., 2013). Due to its inherently low solubility, there is value in creating sustained release dosage forms with itraconazole present in the amorphous phase in order to enhance dissolution and absorption of the drug along the gastrointestinal (GI) tract. This is especially of importance in the distal GI tract regions (i.e. colon), whereby the intestinal fluid volume is reduced (Hatton et al., 2018).

One limitation of FDM printing is, however, the need for the preparation of drug-loaded filaments using HME (Goyanes et al., 2016a, 2017a). The use of HME before the 3D printing process increases the likelihood of drug degradation by the thermal effect. However, the most important disadvantage is the limitation in the use of excipients and drugs to obtain filaments with the appropriate mechanical and physical characteristics for 3D printing (Fuenmayor et al., 2018; Goyanes et al., 2015a). Nowadays, in all pharmaceutical publications relating to FDM 3DP, a significant part of the work is based on the excipient selection and optimisation to create filaments suitable for 3D printing, and there are normally limitations in the drug loading capacity of the selected polymers.

The possibility of avoiding the HME step in FDM 3D printing would be of immense value in pharmaceutical drug development (Awad et al., 2018a). Recently, direct pellet extrusion, a new material extrusion 3DP technology, has been introduced as a potential alternative to FDM printing in the plastics industry (Liu et al., 2017). This technology involves the extrusion of material through a nozzle of the printer in the form of pellets/powder (not filaments) which is directly printed using a single screw extruder. This technology does not require the preparation of filaments using HME and could potentially allow the extrusion of mixtures that would not be possible to be printed by conventional FDM due to the inadequate mechanical characteristics of the filaments, such as being too brittle or too flexible.

As such, the objective of the present work was to explore the use of a novel direct powder extruder 3D printer to prepare sustained release itraconazole printlets (3D printed tablets) present as amorphous solid dispersions using four HPC grades. Printlets (3D printed tablets) were prepared by incorporating therapeutically relevant dosages of itraconazole (selected as a model drug of low solubility) and the effect of the different HPC grades on the characteristics of the printlets were evaluated, paying special attention to the drug phase and dissolution rate.

2. Material and Methods

2.1. Materials

Itraconazole USP grade (Fagron, UK) was used as a model drug (MW 705.64, water solubility: 1–4 ng/mL). Four different grades of HPC (Nippon Soda, Tokyo, Japan) were evaluated: HPC-UL (ultra-low molecular weight, MW 20,000), HPC-SSL (MW 40,000), HPC-SL (MW

Table 1
Composition of the formulations.

Formulation	Itraconazole (%)	HPC-UL (%)	HPC-SSL (%)	HPC-SL (%)	HPC-L (%)	Printing temperature (°C)
Formulation UL	35	65				170
Formulation SSL	35		65			170
Formulation SL	35			65		170
Formulation L	35				65	170

100,000) and HPC-L (MW 140,000). The salts for preparing the buffer dissolution media were purchased from VWR International Ltd., UK.

2.2. Methods

2.2.1. Preparation of drug-loaded itraconazole- HPC dosage forms

For each batch, 8 g of a blend of HPC and itraconazole were manually mixed using a mortar and pestle until no agglomerated particles of drug or polymers were observed. The compositions of the formulations evaluated in this study are listed in Table 1. The prepared mixture was then added to the hopper of the 3D printer extruder. The 3D printer (FabRx, UK) is specifically designed to prepare pharmaceutical products and it can incorporate different exchangeable tools. The selected tool was a direct single-screw powder extruder (FabRx, UK) with a nozzle diameter of 0.8 mm (Fig. 1). The design is based on a single-screw HME however the rotation speed (and hence the extrusion) is controlled by the software of the 3D printer. Furthermore, the extruder nozzle moves in 3 dimensions to create the objects in a layer-by-layer fashion.

AutoCAD 2014 (Autodesk Inc., USA) was used to design the templates of the printlets, exported as a stereolithography (.stl) file into 3D printer software (Repetier host v. 2.1.3, Germany). The .stl format contains only the object surface data, and all the other parameters need to be defined from the Repetier Host software in order to print the desired object. The selected 3D geometry was a cylindrical printlet (10 mm diameter × 3.6 mm height). The printer settings of the software were as follows: Feed 2100 steps/mm, infill 100%, high resolution with brim, without raft and an extrusion temperature of 170 °C, speed while extruding (20 mm/s), speed while travelling (90 mm/s), number of shells (2) and layer height (0.20 mm).

2.2.2. Morphology

The physical dimensions of the printlets were measured using a digital Vernier caliper. Pictures of the devices were taken with a Nikon Coolpix S6150 with the macro option of the menu.

2.2.2.1. Scanning electron microscopy (SEM). Morphology of the extruded feedstock and printlets were evaluated by scanning electron microscopy (SEM) using a Philips XL30 FEG SEM, operating at 20 kV. Samples were placed on double-sided carbon tape, mounted on stubs and sputter coated using a Polaron E5000 machine with Au/Pd. Samples were coated for 1 min prior to imaging.

2.2.3. Determination of the mechanical properties of the printlets

The breaking force of 6 printlets of each type was measured using a traditional tablet hardness tester TBH 200 (Erweka GmbH, Heusenstamm, Germany), whereby an increasing force is applied perpendicular to the tablet axis to opposite sides of a tablet until the printlet fractures.

2.2.4. X-ray powder diffraction (XRPD)

Discs of 23 mm diameter × 1 mm height made from the mixtures of drug and excipient were 3D printed and analysed. Samples of pure itraconazole and the polymers were also analysed. The X-ray powder diffraction patterns were obtained in a Rigaku MiniFlex 600 (Rigaku,

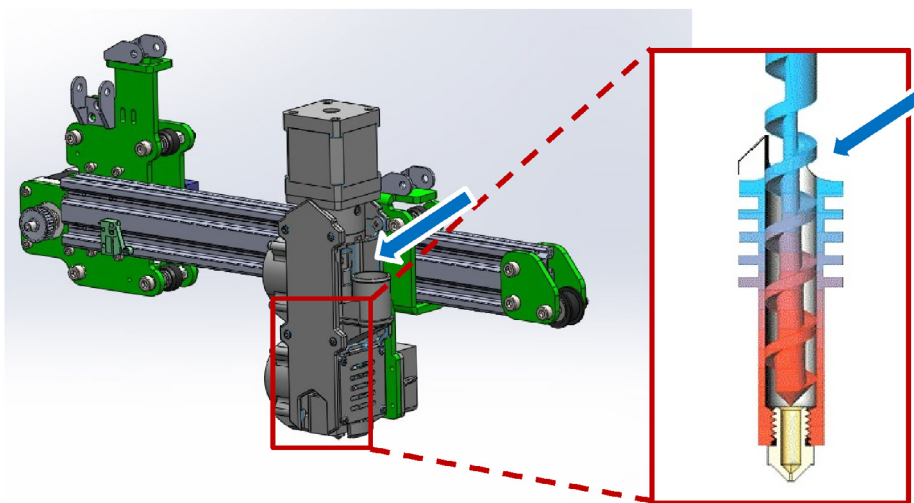


Fig. 1. Design of the nozzle of the direct single-screw powder extruder FabRx 3D printer. The blue arrows indicate the site of addition of the powder.

USA) using a Cu K α X-ray source ($\lambda = 1.5418 \text{ \AA}$). The intensity and voltage applied were 15 mA and 40 kV. The angular range of data acquisition was $3\text{--}60^\circ 2\theta$, with a stepwise size of 0.02° at a speed of $5^\circ/\text{min}$.

2.2.5. Thermal analysis

Differential scanning calorimetry (DSC) and thermogravimetric analysis (TGA) were used to characterise the melting point and degradation profile of the drug. DSC measurements were performed with a Q2000 DSC (TA Instruments, Waters, LLC, U.S.A.) at a heating rate of $10^\circ\text{C}/\text{min}$. Calibration for cell constant and enthalpy was performed with indium ($T_m = 156.6^\circ\text{C}$, $\Delta H_f = 28.71 \text{ J/g}$) according to the manufacturer instructions. Nitrogen was used as a purge gas with a flow rate of $50 \text{ mL}/\text{min}$ for all the experiments. Data were collected with TA Advantage software for Q series (version 2.8.394), and analysed using TA Instruments Universal Analysis 2000. Melting temperature is reported as extrapolated onset unless otherwise stated. TA aluminium pans and lids (Tzero) were used with an average sample mass of $8\text{--}10 \text{ mg}$. For TGA analysis, samples were heated at $10^\circ\text{C}/\text{min}$ in open aluminium pans with a Discovery TGA (TA Instruments, Waters, LLC, U.S.A.). Nitrogen was used as a purge gas with a flow rate of $25 \text{ mL}/\text{min}$. Data collection and analysis were performed using TA Instruments Trios software and percent mass loss or onset temperature were calculated.

2.2.6. Determination of drug loading

One printlet (approximately 300 mg) of each formulation was placed in a volumetric flask with 1:1 ethanol:acetonitrile mixture (100 mL) under magnetic stirring until complete dissolution ($n = 2$). Samples of the solutions were then filtered through $0.22 \mu\text{m}$ filter (Millipore Ltd., Ireland) and the concentration of drug determined with high-performance liquid chromatography (HPLC; Hewlett-Packard 1050 Series HPLC system, Agilent Technologies, U.K.).

The validated HPLC assay entailed injecting $10 \mu\text{L}$ samples for analysis using a mobile phase, consisting of isocratic system composed of 70% acetonitrile (ACN) and 30% water pumped at a flow rate of $1 \text{ mL}/\text{min}$, through an Eclipse plus $5 \mu\text{m}$ C18 column, $150 \times 4.6 \text{ mm}$ (Phenomenex, U.K.) maintained at 40°C . The eluent was screened at a wavelength of 260 nm . The retention time of itraconazole was found to be at approximately 4 min .

2.2.7. Dissolution testing

Dissolution profiles were obtained using a USP-II apparatus (Model PTWS, Pharmatest, Germany). In each assay, the printlets were placed at the bottom of the vessel in simulated gastric fluid ($0.2\% \text{ w/v}$ sodium

chloride in 0.1 N HCl , $\text{pH } 1.2$, 900 mL) under constant paddle stirring (100 rpm) at 37°C . During the dissolution test, 5 mL samples of itraconazole were removed and filtered through $0.22 \mu\text{m}$ filters and drug concentration was determined HPLC. Tests were conducted in triplicate. Data are reported throughout as mean \pm standard deviation.

3. Results and discussion

A single-screw direct powder extruder 3D printer that was originally designed for printing with polylactic acid (PLA) or acrylonitrile butadiene styrene (ABS) pellets was adapted and used for the first time to print with pharmaceutical formulations; a mixture of drug and excipients. Itraconazole printlets (3D printed tablets) were successfully printed with four different HPC grades and itraconazole using the 3D printer for all the formulations listed in Table 1. The mixture was added into the hopper of the printer using a small spatula to push the material inside the single-screw extruder. The design of the extruder in a vertical orientation facilitates the flow of the powder into the screw and minimises the presence of air bubbles during the printing process. After the printing of each formulation, the extruder was removed from the printing platform and the screw dismounted and washed to avoid cross-contamination between the different formulations.

All of the HPC polymers were found to be very suitable materials for direct powder 3D printing without the need for including other pharmaceutical excipients. The mixtures incorporating 35% itraconazole (Table 1) were selected to obtain cylindrical printlets with dimensions of $10 \text{ mm diameter} \times 3.6 \text{ mm height}$ with a final dose close to 100 mg of itraconazole. The printing time per printlet was similar to that using FDM technology ($2\text{--}3 \text{ min}$ per printlet). The fact that is not necessary to undertake a preliminary HME step makes the direct powder printing process much simpler and faster compared to HME coupled with FDM printing. Another advantage of this innovative technology is that small amounts of mixtures of drug and excipients can be 3D printed (8 g in this study), reducing the amount of wastage, since the material can be directly printed without intermediate steps where part of the material can be lost. The reduced amount of material needed and the quick preparation of formulations could make this technology especially suited to preclinical studies, where only small amounts of drugs may be available and not many resources are allocated for the preparation of oral dosage forms. Using direct powder extrusion it would be possible to quickly and easily prepare oral formulations of different dose strengths using small amounts of raw material (compared to other technologies like HME coupled with FDM printing).

All of the printlets showed a cylindrical shape and good adhesion between the printed layers (Fig. 2). Regarding the surface



Fig. 2. Pictures of itraconazole printlets, from left to right: Formulation UL, SSL, SL and L. Units are cm.

characteristics, the smoothness of the printlets increased when reducing the molecular weight, with smoothness following this rank order: HPC-UL > SSL > SL > L. The printlets prepared with the higher molecular weight HPC-SL and HPC-L show small particles on the surface of the printlets.

SEM pictures of the cross sections of the printlets provide visual confirmation of the different effects of the polymers on the printlets, even though the same printing parameters were used (Fig. 3). The images show that HPC-UL and HPC-SSL undergoes a more intense melting indicated by the smoother surface and cross section (Fig. 3A and B). However, the polymers HPC-SL and HPC-L produced a rougher surface and cross section.

The printlets showed good uniformity in physical dimensions (Table 2), with the size of the printlets being slightly bigger than the theoretical size (3.6 mm × 10 mm), with a mean height ranging from 3.73 mm to 3.86 mm and the diameter from 10.24 mm to 10.83 mm. The mean mass of the formulations ranged from 309 mg to 348 mg; this variability could be attributable to the different flow properties of the different polymer grades, which leads to different amounts of mixture being deposited by the extruder.

All of the formulations were mechanically strong and showed appropriate properties for handling and packing. The printlet breaking force data show values higher than 100 N for all formulations up to the value of 483 N for Formulations L, which represents the maximum value measurable by the tablet hardness tester. These values are comparable to those previously reported from printlets prepared by conventional FDM printing (Goyanes et al., 2015a, 2016b).

It is of importance to demonstrate the stability of the itraconazole during the printing process using the single-screw direct powder extruder. TGA was used to determine the degradation profile of the drug and the excipients (Fig. 4). All the HPC polymers were found to be stable up to at least 250 °C, while the drug did not show any significant degradation under 250 °C. TGA data predicted that all the components would remain stable and no degradation of the drugs and excipients is likely to occur at the printing temperature (170 °C), hence, itraconazole is expected to be stable in the formulations while printing. Chemical integrity of the drug in the final printlets was analysed using HPLC (Table 2). The drug content values were in agreement with the theoretical drug loading in all the printlets (35% w/w), confirming that no significant drug loss occurred during the printing process.

DSC and XRPD were used to examine the solid state of the drug in the final formulations. It is apparent that itraconazole pure material melts around 170 °C (Fig. 5), while HPC polymers did not show any endothermic peaks, indicative of the amorphous form. The DSC data of the itraconazole-loaded HPC – L, SL and SSL printlets each showed a melting endotherm at about 170 °C, indicating that itraconazole is (at least partially) in its crystalline form. The formulation UL shows no evidence of melting around 170 °C, indicating that the drug is molecularly dispersed within the polymer matrix as a solid solution or dispersion.

X-ray diffractograms of the drug, excipients and final formulation were studied (Fig. 6). Itraconazole showed sharp peaks indicative for the crystalline form of the drug, while HPC polymers showed wide halos that are representative for their amorphous structure. The

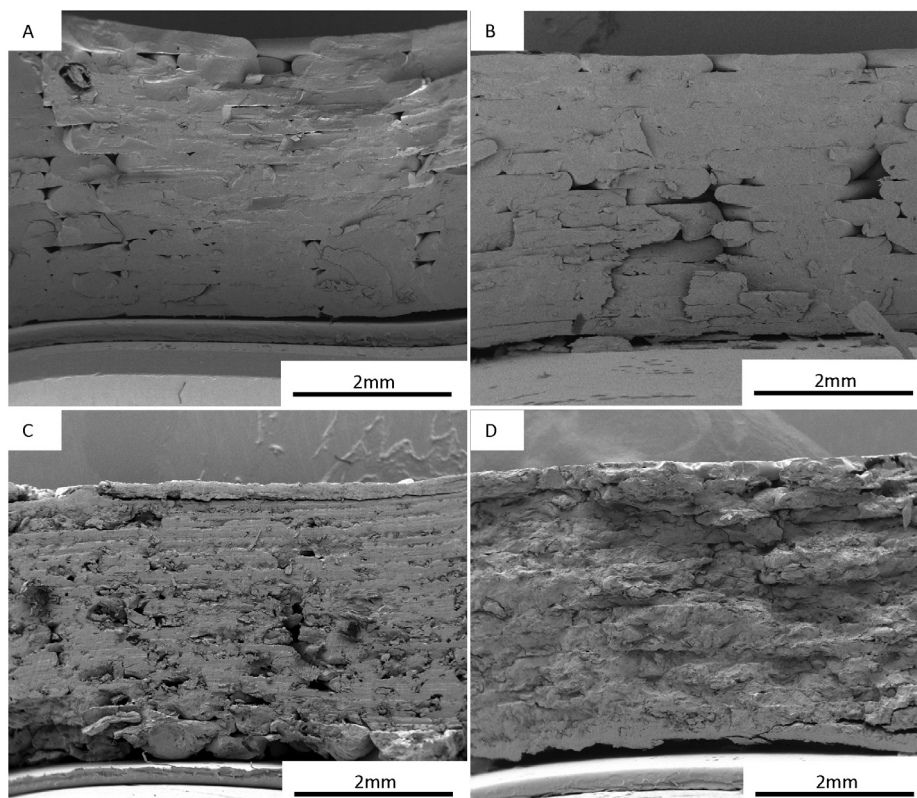


Fig. 3. SEM images of the cross sections of the printlets: A) Formulation UL, B) Formulation SSL, C) Formulation SL, and D) Formulation L.

Table 2
Characteristics of the printlets.

Formulation	Diameter (mm)	Height (mm)	Weight (mg)	Breaking force (N)	Itraconazole loading (%)
Formulation UL	10.53 ± 0.31	3.79 ± 0.15	348.9 ± 39.5	148.0 ± 12.5	34.70 ± 0.83
Formulation SSL	10.24 ± 0.25	3.73 ± 0.07	309.9 ± 45.9	104.7 ± 84.3	33.48 ± 0.65
Formulation SL	10.6 ± 0.41	3.84 ± 0.12	323.7 ± 43.3	343.3 ± 71.0	35.17 ± 0.63
Formulation L	10.83 ± 0.52	3.86 ± 0.07	339.2 ± 52.9	483.5 ± 0.7	33.99 ± 0.32

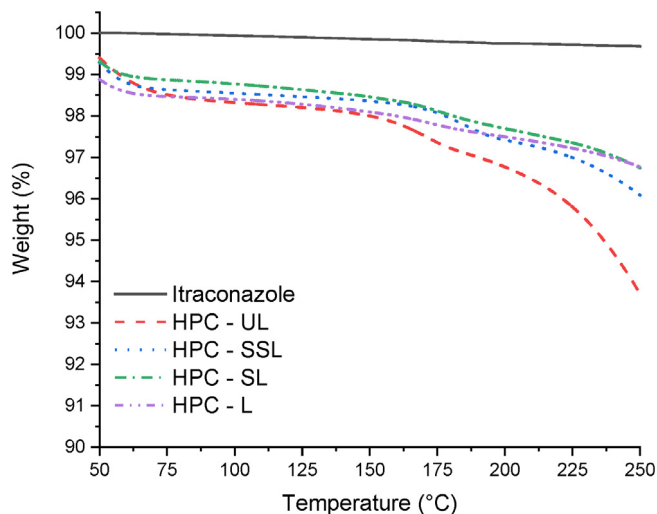


Fig. 4. TGA thermal traces for itraconazole raw material and HPC polymers.

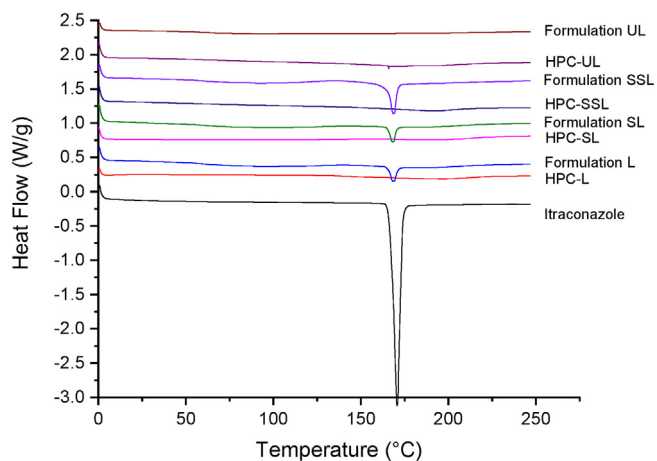


Fig. 5. DSC thermograms of pure itraconazole and individual polymers prior to printing and the different printlet formulations.

absence of the sharp peaks of itraconazole in the diffractograms of the formulations, suggests that the drug is in the amorphous form in the formulation, or if any fraction of it is crystalline then it is beyond the limit of detection of the instrument (usually 5% w/w is typical).

The results of XRD and DSC suggest that the drug is amorphous in formulations prepared with HPC – UL and partially amorphous in Formulations L, SL, and SSL. This implies that HPC polymers enable the transition of the drug from the crystalline state to the amorphous state in all the formulations, facilitated by the fact that the printing temperature is equal to the melting point of the pure drug (170 °C). From the XRD and DSC data it is clear that the HPC – UL increases the amorphous transition at a higher rate than the other polymers, probably due to the lower molecular weight (and hence viscosity) of the polymer, which may facilitate the inclusion of the drug molecules into the polymer.

Drug dissolution studies from printlets incorporating 100 mg of

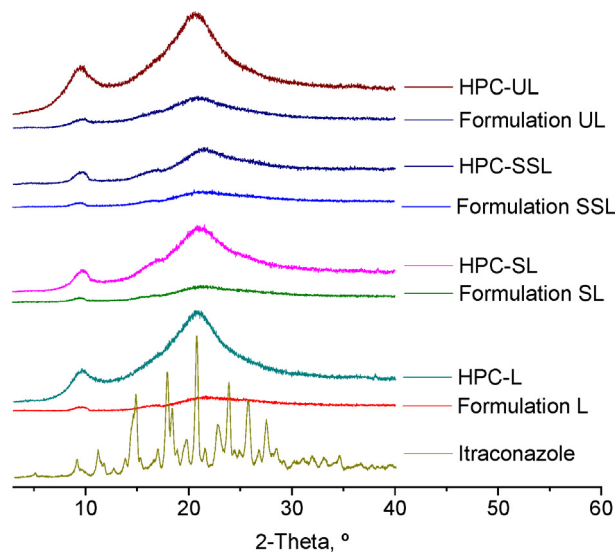


Fig. 6. X-ray powder diffractograms of pure components and 3D printed disc of the four formulations.

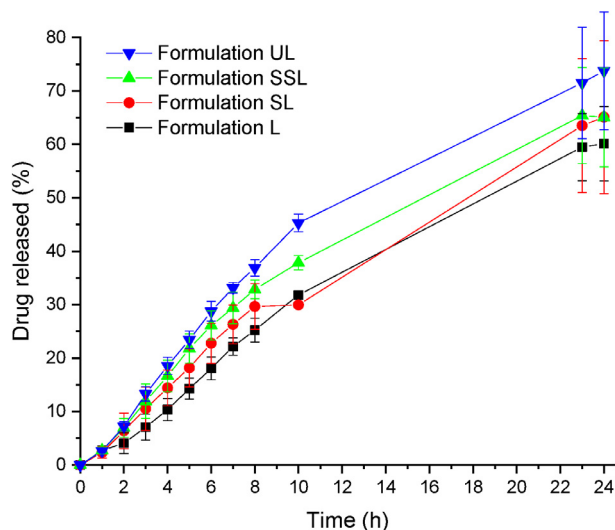


Fig. 7. Dissolution profiles of itraconazole printlets with a dose equivalent of 100 mg.

itraconazole were performed within 0.1 N HCl with 0.2% NaCl, simulating gastric conditions (Fig. 7). All the formulations show a similar zero order drug release during the first 8 h. After 24 h, the drug release achieved was 60.1%, 65.1%, 65.7% and 73.8% for Formulation L, Formulation SL, Formulation SSL and Formulation UL respectively. Formulation UL, which has the lowest molecular weight, showed the fastest release compared with the other HPC grades used, with Formulation L (with the highest molecular weight) showing the slowest release. For all formulations, a sustained release profile was achieved enabling drug release to occur over more than 24 h.

The drug dissolution profiles from the printlets showed a drug

concentration ~20 times higher than itraconazole solubility 4.57 µg/mL (Konnerth et al., 2018; Miller et al., 2008). As a sustained release is achieved, the presence of itraconazole in the amorphous phase would enable the enhanced dissolution and absorption of the drug along the gastrointestinal (GI) tract, which is of importance in the distal GI tract regions (i.e. colon) whereby the intestinal fluid volume is lower (Hatton et al., 2018). The observed solubility enhancement is higher than obtained using an alternative technology (nanosuspension technology) with the same HPC grades and similar drug/HPC ratio, which released only about 20% itraconazole (Konnerth et al., 2018). This shows the superiority of the melting process to obtain solid amorphous dispersions, and confirms the use of the powder extrusion 3D printing technology to increase the drug solubility of the formulations. HPC, a hydrophilic carrier, may facilitate water penetration and wetting of the hydrophobic itraconazole, which is found as amorphous solid dispersion. The reduction on the molecular weight of the polymer may increase the wettability of the whole system leading to increased drug release.

The dissolution enhancement of itraconazole using HME has been previously reported by combining the drug with mixtures of different excipients including hypromellose acetate succinate-L, polyethylene oxide and poloxamer (Lang et al., 2014) or polyethylene glycol, polyvinyl acetate and polyvinylcaprolactame-based graft copolymer, cyclodextrins and superdisintegrants (Thiry et al., 2017). The solubility enhancement and the extent of itraconazole supersaturation in vitro directly correlates with the in vivo oral absorption of the drug and bioavailability (Miller et al., 2008). It is worthy to mention that in the previous studies, the evaluated formulations were the extrudates (granulates) obtained from the hot melt extruder that should be considered as intermediate products, since they have to be filled into capsules or sachets or compressed into tablets. However, in this study the formulations tested are the printlets that do not require later manufacturing process for administration. Additionally, the drug release can be tuned by the selected 3D computer model design or by changing parameters like the surface/volume ratio (Martinez et al., 2018; Sadia et al., 2018).

The use of this innovative direct powder extrusion 3D printing technology with HPC (especially HPC – UL) has been successful in not only solubilising the very poorly soluble drug, but also producing printlets in a single step process. This innovative 3D printing technology obviates the need for the expensive and laborious HME step and makes the technology more accessible for research and facilitates the preparation of formulations as amorphous dispersions for preclinical and clinical evaluation of drugs using small amounts of drugs and excipients.

4. Conclusion

Preparation of printlets containing itraconazole-HPC by single-screw direct powder extrusion 3D printing has been successfully demonstrated for the first time. All of the printlets showed good mechanical and physical characteristics, and a drug release higher than the solubility of the drug. The printlets prepared with the ultra-low molecular grade hydroxypropylcellulose (HPC – UL) showed faster drug release than the other HPC grades, attributed to fact that itraconazole is found as an amorphous solid dispersion.

This work demonstrates that this innovate technology can overcome one of the major disadvantages of fused deposition modelling (FDM) 3D printing by avoiding the preparation of filaments by hot melt extrusion. This single-step new technology could revolutionise the preparation of amorphous solid dispersions as final formulations and it may be especially suited for preclinical studies, where the amount of drug is often limited.

Declaration of Competing Interest

None.

Acknowledgements

The authors thank 3D Limitless for their technical expertise with the development of the 3D printing system, and for their continual support during the study. The authors also thank the Engineering and Physical Sciences Research Council (EPSRC) UK for their financial support towards this manuscript (EP/L01646X).

Appendix A. Supplementary data

Supplementary data to this article can be found online at <https://doi.org/10.1016/j.ijpharm.2019.118471>.

References

- Alhijaj, M., Belton, P., Qi, S., 2016. An investigation into the use of polymer blends to improve the printability of and regulate drug release from pharmaceutical solid dispersions prepared via fused deposition modeling (FDM) 3D printing. *Eur. J. Pharm. Biopharm.* 108, 111–125.
- Alhnan, M.A., Okwuosa, T.C., Sadia, M., Wan, K.W., Ahmed, W., Arafat, B., 2016. Emergence of 3D printed dosage forms: opportunities and challenges. *Pharm. Res.* 33, 1817–1832.
- Arafat, B., Qinna, N., Cieszyńska, M., Forbes, R.T., Alhnan, M.A., 2018a. Tailored on demand anti-coagulant dosing: an in vitro and in vivo evaluation of 3D printed purpose-designed oral dosage forms. *Eur. J. Pharm. Biopharm.* 128, 282–289.
- Arafat, B., Wojsz, M., Isreb, A., Forbes, R.T., Isreb, M., Ahmed, W., Arafat, T., Alhnan, M.A., 2018b. Tablet fragmentation without a disintegrant: a novel design approach for accelerating disintegration and drug release from 3D printed cellulose tablets. *Eur. J. Pharm. Sci.* 118, 191–199.
- Ashbee, H.R., Barnes, R.A., Johnson, E.M., Richardson, M.D., Gorton, R., Hope, W.W., 2013. Therapeutic drug monitoring (TDM) of antifungal agents: guidelines from the British Society for Medical Mycology. *J. Antimicrob. Chemother.* 69, 1162–1176.
- ASTM, 2012. Standard Terminology for Additive Manufacturing Technologies. F2792 – 12a.
- Awad, A., Fina, F., Trenfield, S.J., Patel, P., Goyanes, A., Gaisford, S., Basit, A.W., 2019. 3D printed pellets (Miniprintlets): a novel, multi-drug, controlled release platform technology. *Pharmaceutics* 11, 148.
- Awad, A., Trenfield, S.J., Gaisford, S., Basit, A.W., 2018a. 3D printed medicines: a new branch of digital healthcare. *Int. J. Pharm.* 548, 586–596.
- Awad, A., Trenfield, S.J., Goyanes, A., Gaisford, S., Basit, A.W., 2018b. Reshaping drug development using 3D printing. *Drug Discovery Today* 23, 1547–1555.
- Barnatt, C., 2016. 3D Printing. Barnatt, C., UK.
- Barone, J.A., Koh, J., Bierman, R., Colaizzi, J., Swanson, K., Gaffar, M., Moskovitz, B., Mechlinski, W., Van de Velde, V., 1993. Food interaction and steady-state pharmacokinetics of itraconazole capsules in healthy male volunteers. *Antimicrob. Agents Chemother.* 37, 778–784.
- Basit, A.W., Gaisford, S., 2018. 3D Printing of Pharmaceuticals, first ed. Springer International Publishing DOI: 10.1007/978-3-319-90755-0.
- Fina, F., Goyanes, A., Madla, C.M., Awad, A., Trenfield, S.J., Kuek, J.M., Patel, P., Gaisford, S., Basit, A.W., 2018a. 3D printing of drug-loaded gyroid lattices using selective laser sintering. *Int. J. Pharm.* 547, 44–52.
- Fina, F., Madla, C.M., Goyanes, A., Zhang, J., Gaisford, S., Basit, A.W., 2018b. Fabricating 3D printed orally disintegrating printlets using selective laser sintering. *Int. J. Pharm.* 541, 101–107.
- Fuenmayor, E., Forde, M., Healy, A.V., Devine, D.M., Lyons, J.G., McConville, C., Major, I., 2018. Material considerations for fused-filament fabrication of solid dosage forms. *Pharmaceutics* 10, 44.
- Genina, N., Boetker, J.P., Colombo, S., Harmankaya, N., Rantanen, J., Bohr, A., 2017. Anti-tuberculosis drug combination for controlled oral delivery using 3D printed compartmental dosage forms: from drug product design to in vivo testing. *J. Controlled Release* 268, 40–48.
- Goole, J., Amighi, K., 2016. 3D printing in pharmaceutics: a new tool for designing customized drug delivery systems. *Int. J. Pharm.* 499, 376–394.
- Goyanes, A., Buanz, A.B., Hatton, G.B., Gaisford, S., Basit, A.W., 2015a. 3D printing of modified-release aminosalicylate (4-ASA and 5-ASA) tablets. *Eur. J. Pharm. Biopharm.* 89, 157–162.
- Goyanes, A., Det-Amornrat, U., Wang, J., Basit, A.W., Gaisford, S., 2016a. 3D scanning and 3D printing as innovative technologies for fabricating personalized topical drug delivery systems. *J. Controlled Release* 234, 41–48.
- Goyanes, A., Fernandez-Ferreiro, A., Majeed, A., Gomez-Lado, N., Awad, A., Luaces-Rodriguez, A., Gaisford, S., Aguiar, P., Basit, A.W., 2018. PET/CT imaging of 3D printed devices in the gastrointestinal tract of rodents. *Int. J. Pharm.* 536, 158–164.
- Goyanes, A., Fina, F., Martorana, A., Sedough, D., Gaisford, S., Basit, A.W., 2017a. Development of modified release 3D printed tablets (printlets) with pharmaceutical excipients using additive manufacturing. *Int. J. Pharm.* 527, 21–30.
- Goyanes, A., Kobayashi, M., Martinez-Pacheco, R., Gaisford, S., Basit, A.W., 2016b.

- Fused-filament 3D printing of drug products: microstructure analysis and drug release characteristics of PVA-based caplets. *Int. J. Pharm.* 514, 290–295.
- Goyanes, A., Martinez, P.R., Buanz, A., Basit, A., Gaisford, S., 2015b. Effect of geometry on drug release from 3D printed tablets. *Int. J. Pharm.* 494, 657–663.
- Goyanes, A., Scarpa, M., Kamlow, M., Gaisford, S., Basit, A.W., Orlu, M., 2017b. Patient acceptability of 3D printed medicines. *Int. J. Pharm.* 530, 71–78.
- Goyanes, A., Wang, J., Buanz, A., Martinez-Pacheco, R., Telford, R., Gaisford, S., Basit, A.W., 2015c. 3D printing of medicines: engineering novel oral devices with unique design and drug release characteristics. *Mol. Pharm.* 12, 4077–4084.
- Hatton, G.B., Madla, C.M., Rabbie, S.C., Basit, A.W., 2018. All disease begins in the gut: Influence of gastrointestinal disorders and surgery on oral drug performance. *Int. J. Pharm.* 548, 408–422.
- Khaled, S.A., Burley, J.C., Alexander, M.R., Yang, J., Roberts, C.J., 2015a. 3D printing of five-in-one dose combination polypill with defined immediate and sustained release profiles. *J. Controlled Release* 217, 308–314.
- Khaled, S.A., Burley, J.C., Alexander, M.R., Yang, J., Roberts, C.J., 2015b. 3D printing of tablets containing multiple drugs with defined release profiles. *Int. J. Pharm.* 494, 643–650.
- Konnerth, C., Braig, V., Stoyanov, E., Lee, G., Peukert, W., 2018. Efficient drug solubility enhancement by using ultra-low molecular weight HPC. *AAPS PharmSci* 360 T1330-10-079.
- Lang, B., McGinity, J.W., Williams 3rd, R.O., 2014. Dissolution enhancement of itraconazole by hot-melt extrusion alone and the combination of hot-melt extrusion and rapid freezing—effect of formulation and processing variables. *Mol. Pharm.* 11, 186–196.
- Liang, K., Carmone, S., Brambilla, D., Leroux, J.-C., 2018. 3D printing of a wearable personalized oral delivery device: a first-in-human study. *Sci. Adv.* 4, eaat2544.
- Liu, X., Chi, B., Jiao, Z., Tan, J., Liu, F., Yang, W., 2017. A large-scale double-stage-screw 3D printer for fused deposition of plastic pellets. *J. Appl. Polym. Sci.* 134, 45147.
- Madla, C.M., Trenfield, S.J., Goyanes, A., Gaisford, S., Basit, A.W., 2018. 3D printing technologies, implementation and regulation: an overview. In: Basit, A.W., Gaisford, S. (Eds.), *3D Printing of Pharmaceuticals*. Springer International Publishing, pp. 21–40.
- Martinez, P.R., Goyanes, A., Basit, A.W., Gaisford, S., 2018. Influence of geometry on the drug release profiles of stereolithographic (SLA) 3D-printed tablets. *AAPS PharmSciTech* 19, 3355–3361.
- Melocchi, A., Parietti, F., Maroni, A., Foppoli, A., Gazzaniga, A., Zema, L., 2016. Hot-melt extruded filaments based on pharmaceutical grade polymers for 3D printing by fused deposition modeling. *Int. J. Pharm.* 509, 255–263.
- Miller, D.A., DiNunzio, J.C., Yang, W., McGinity, J.W., Williams 3rd, R.O., 2008. Enhanced in vivo absorption of itraconazole via stabilization of supersaturation following acidic-to-neutral pH transition. *Drug Dev. Ind. Pharm.* 34, 890–902.
- Palo, M., Holländer, J., Suominen, J., Yliruusi, J., Sandler, N., 2017. 3D printed drug delivery devices: perspectives and technical challenges. *Expert Rev. Med. Devices* 14, 685–696.
- Pietrzak, K., Isreb, A., Alhnan, M.A., 2015. A flexible-dose dispenser for immediate and extended release 3D printed tablets. *Eur. J. Pharm. Biopharm.* 96, 380–387.
- Robles-Martinez, P., Xu, X., Trenfield, S.J., Awad, A., Goyanes, A., Telford, R., Basit, A.W., Gaisford, S., 2019. 3D printing of a multi-layered polypill containing six drugs using a novel stereolithographic method. *Pharmaceutics* 11, 274.
- Sadia, M., Arafat, B., Ahmed, W., Forbes, R.T., Alhnan, M.A., 2018. Channelled tablets: an innovative approach to accelerating drug release from 3D printed tablets. *J. Controlled Release* 269, 355–363.
- Thiry, J., Kok, M.G.M., Collard, L., Frère, A., Krier, F., Fillet, M., Evrard, B., 2017. Bioavailability enhancement of itraconazole-based solid dispersions produced by hot melt extrusion in the framework of the Three Rs rule. *Eur. J. Pharm. Sci.* 99, 1–8.
- Trenfield, S.J., Awad, A., Goyanes, A., Gaisford, S., Basit, A.W., 2018a. 3D printing pharmaceuticals: drug development to frontline care. *Trends Pharmacol. Sci.* 39, 440–451.
- Trenfield, S.J., Goyanes, A., Telford, R., Wilsdon, D., Rowland, M., Gaisford, S., Basit, A.W., 2018b. 3D printed drug products: non-destructive dose verification using a rapid point-and-shoot approach. *Int. J. Pharm.* 549, 283–292.
- Trenfield, S.J., Xian Tan, H., Awad, A., Buanz, A., Gaisford, S., Basit, A.W., Goyanes, A., 2019. Track-and-trace: novel anti-counterfeit measures for 3D printed personalised drug products using smart material inks. *Int. J. Pharm.* 567, 118443.
- Vithani, K., Goyanes, A., Jannin, V., Basit, A.W., Gaisford, S., Boyd, B.J., 2019. An overview of 3D printing technologies for soft materials and potential opportunities for lipid-based drug delivery systems. *Pharm. Res.* 36, 4.
- Zema, L., Melocchi, A., Maroni, A., Gazzaniga, A., 2017. Three-dimensional printing of medicinal products and the challenge of personalized therapy. *J. Pharm. Sci.* 106, 1697–1705.